Title

Glycine homeostasis requires reverse SHMT flux.

Journal

Cell Metabolism, 36(1)

Authors

McBride, Matthew
Hunter, Craig
Zhang, Zhaoyue
et al.

Publication Date

2024-01-02

DOI

10.1016/j.cmet.2023.12.001

Peer reviewed

HHS Public Access

Author manuscript

Cell Metab. Author manuscript; available in PMC 2025 March 10.

Published in final edited form as:

Cell Metab. 2024 January 02; 36(1): 103–115.e4. doi:10.1016/j.cmet.2023.12.001.

Glycine homeostasis requires reverse SHMT flux

Matthew J. McBride[1,2,3], **Craig J. Hunter**[1,2,3], **Zhaoyue Zhang**[1,2], **Tara TeSlaa**[1,2], **Xincheng Xu**[1,2], **Gregory S. Ducker**[1,2], **Joshua D. Rabinowitz**[*,1,2,3]

[1]Department of Chemistry, Princeton University, Princeton NJ, USA

[2]Lewis-Sigler Institute of Integrative Genomics, Princeton University, Princeton NJ, USA

[3]Ludwig Institute for Cancer Research, Princeton University, Princeton NJ, USA

SUMMARY

The folate-dependent enzyme serine hydroxymethyltransferase (SHMT) reversibly converts serine into glycine and a tetrahydrofolate-bound one-carbon unit. Such one-carbon unit production plays a critical role in development, the immune system, and cancer. Using rodent models, here we show that the whole-body SHMT flux acts to net consume rather than produce glycine. Pharmacological inhibition of whole-body SHMT1/2 and genetic knockout of liver SHMT2 elevated circulating glycine levels up to eight-fold. Stable isotope tracing revealed that the liver converts glycine to serine, which is then converted by serine dehydratase into pyruvate and burned in the tricarboxylic acid cycle. In response to diets deficient in serine and glycine, de novo biosynthetic flux was unaltered but SHMT2- and serine dehydratase-mediated catabolic flux was lower. Thus, glucose-derived serine synthesis does not respond to systemic demand. Instead, circulating serine and glycine homeostasis is maintained through variable consumption, with liver SHMT2 a major glycine-consuming enzyme.

INTRODUCTION

The non-essential amino acids serine and glycine are circulating nutrients required by mammalian tissues to support biosynthesis of proteins, nucleotides, and lipids[1]. Homeostasis of these amino acids requires balancing production (by dietary intake and de novo synthesis) with consumption (by biosynthetic and catabolic pathways)[2]. Depletion of circulating glycine and thus disrupted homeostasis is a hallmark of metabolic syndrome[3,4].

[*]Lead Contact and corresponding author: joshr@princeton.edu.

AUTHOR CONTRIBUTIONS

M.J.M and J.D.R. conceived and designed the study. M.J.M performed experiments and data analysis. C.H. performed catheterization surgeries and tail vein injections. Z.Z, T.T., and X.X assisted with SHIN2 experiments. G.D. provided critical insights for project conceptualization. M.J.M and J.D.R. wrote the manuscript.

DECLARATION OF INTERESTS

J.D.R. is a member of the Rutgers Cancer Institute of New Jersey and the University of Pennsylvania Diabetes Research Center; a co-founder, stockholder and director of Raze Therapeutics and Farber Partners; and an advisor and stockholder in in Empress Therapeutics, Bantam Pharmaceuticals, Colorado Research Partners, Rafael Pharmaceuticals, Barer Institute, and L.E.A.F. Pharmaceuticals. G.D. and J.D.R. are co-inventors of SHIN2 and related SHMT inhibitors, which have been patented by Princeton University. The remaining authors declare no competing interests.

De novo synthesis of both serine and glycine begins from the glycolytic intermediate 3-phosphoglycerate via three enzymatic reactions initiated by phosphoglycerate dehydrogenase (PHGDH) to make serine[5-7]. Serine is then transformed by serine hydroxymethyltransferase in the cytoplasm (SHMT1) or mitochondria (SHMT2) to glycine and a one-carbon (1C) unit bound to tetrahydrofolate (THF)[8]. Glycine can also be synthesized from threonine catabolism, though this pathway is lost in humans[9]. In cell lines, depletion of serine and glycine from culture media drives an increase in their de novo synthesis from glucose[10,11]. This is consistent with intracellular de novo synthesis of non-essential amino acids increasing when supply from the extracellular environment decreases.

A major function of serine and glycine is to provide 1C units for purine, thymidine, and methionine synthesis[12-14]. This can occur through serine conversion to glycine plus a 1C unit by SHMT or through glycine conversion to CO_2 plus a 1C unit by glycine cleavage system (GCS)[15]. Among the two SHMT isozymes, SHMT2 is more functionally important. Genetic deletion of either SHMT2 or GCS results in development defects prototypical of folate or 1C deficiency[16,17]. Outside of development, SHMT2 is a key driver of T cell activation and cancer cell proliferation[18,19].

While most interest in serine and glycine metabolism has focused on their importance as biosynthetic precursors, there is also need to catabolize these amino acids to prevent excessive accumulation. Classically, serine is catabolized to pyruvate by the liver-specific enzyme serine dehydratase[20] and to glycine by SHMT1/2 with glycine subsequently cleared by GCS in the liver[21,22]. Humans with a biallelic loss-of-function mutation in GCS develop non-ketotic hyperglycinemia (NKH) characterized by plasma glycine concentrations up to nine times greater than normal[23]. A third of these patients do not to survive a full year and glycine level correlates with disease severity. Those patients that do reach infancy have neurological impairments that include seizures and diminished psychomotor development.

While SHMT2 is reversible and so can consume glycine and a 1C unit to produce serine, evidence to date suggested that all functional flux was in the forward (i.e. serine-consuming) direction. Surprisingly, however, when we tested pharmacological dual SHMT1/2 inhibitors in mice, rather than seeing glycine depletion as expected, we observed massive elevations. Combining mouse genetics, metabolomics, and tracing, we show that a major path of systemic glycine consumption is liver conversion to serine via SHMT2. This serine can then be further converted by serine dehydratase to pyruvate which can then be oxidized in the TCA cycle. We additionally explore how systemic serine and glycine homeostasis is achieved. Our data support a model of homeostasis where de novo synthesis is independent of dietary supply. Instead, consumption rates, including via the liver SHMT2 pathway, change in proportion to circulating levels.

RESULTS

Loss of hepatic SHMT2 elevates serum glycine

Classically, serine is synthesized from the glycolytic intermediate 3-phosphoglycerate via the PHGDH pathway, and catabolized by the enzyme serine dehydratase[7,20], whose

expression is restricted primarily to liver (Figure S1A). Glycine is synthesized from serine via the folate-dependent enzyme serine hydroxymethyltransferase, and catabolized by another folate-dependent enzyme, the glycine cleavage system (Figure 1A, Figure S1B). We treated mice with vehicle or a dual SHMT1/2 small molecule inhibitor (SHIN2) by intravenous infusion for 12 hours[24]. Serum and liver samples collected following treatment was analyzed by liquid chromatography-mass spectrometry (LC-MS). Rather than suppressing glycine levels, SHIN2 treatment increased circulating glycine from ~400 μM to over 3 mM (Figure 1B, Figure S1C, Table S1). The other strongest metabolite changes in both serum and liver were glycine-containing metabolites, such as acetylglycine and longer-chain acylglycines (Figure 1B, Figure S1D-E, Table S1). Thus, rather than being a net source of circulating glycine, SHMT1/2 appears to be a major glycine consumer.

As small molecules can have off target effects, we turned to genetics to validate this finding and identify the isozyme and tissue responsible for this SHMT-mediated glycine consumption. Whole-body SHMT1 knockout has only modest phenotypes with no reported changes in circulating glycine levels, while whole-body SHMT2 knockout is embryonic lethal in mice[16,25,26]. Thus, we prioritized SHMT2, and generated a SHMT2-floxed mouse ($Shmt2^{flox/flox}$ C57BL/6) for this purpose[27].

To explore the most relevant tissue(s) in which to knockout SHMT2, we infused U13C-glycine systemically in mice and measured serine labeling in different tissues and in the circulation. We hypothesized that serine labeling from circulating glycine would be high in the tissue(s) doing the bulk of reverse SHMT flux. Consistent with this, we observed serine labeling from the infused U13C-glycine in both liver and kidney higher than in the circulation, while labeling in all other tissues was lower than in the circulation (Figure 1C, Figure S1F). Higher serine labeling in a tissue than the circulation cannot occur by tissue uptake of labeled serine made elsewhere in the body, and thus indicates serine production from glycine within that tissue compartment. Thus liver and/or kidney are responsible for systemic glycine to serine flux. As both SHMT2 and the major serine catabolic enzyme serine dehydratase (SDS) are most highly expressed in liver (Figure 1D, Figure S1A), we prioritized liver. Using AAV8 viral infection, we induced liver-specific Cre expression to knockout SHMT2 in $Shmt2^{flox/flox}$ C57BL/6 mice and collected serum and liver tissue for metabolomics (Figure S1G). Similar to SHIN2 treatment, liver-specific SHMT2 knockout dramatically elevated glycine and related metabolites in serum and liver, while serine levels were maintained (Figure 1E-G, Figure S1H-J, Table S1).

As expected, whole-body SHMT1 knockout had no effect on circulating glycine levels (Figure 1G). Knockout of the canonical glycine-catabolic enzyme, glycine decarboxylase (GLDC) of the glycine cleavage system, in a liver-specific manner resulted in similar circulating glycine elevation to liver-specific SHMT2 loss[28] (Figure 1G, Figure S1K). Thus, glycine homeostasis requires both the glycine cleavage system and reverse flux through liver SHMT2.

Glycine is converted to serine for hepatic clearance by TCA cycle oxidation

Reverse SHMT2 flux consumes glycine and a 1C unit to generate serine. In the liver, serine dehydratase can convert serine to pyruvate for consumption by TCA cycle oxidation (Figure

2A, Figure S1A). Based on known major routes of serine clearance, serine catabolism by serine dehydratase is the only route that produces pyruvate[29-31]. To determine the fate of circulating glycine, we infused U13C-glycine in rats and collected arterial and site-specific venous serum samples, which were used to measure metabolite concentrations and labeling by LC-MS (Figure 2B). In rat, the liver net consumed both serine and glycine, as evidenced by lower concentrations in the hepatic vein than incoming blood supply to the liver (blood feeding into the liver is roughly 22% from the arterial circulation and 78% from the portal vein) (Figure S2A-B)[32]. Moreover, the liver catabolized glycine to pyruvate to lactate, as evidenced by increased M+2 lactate labeling in the hepatic vein from U13C-glycine infusion (Figure 2C). Our observed glycine and serine turnover fluxes in rats are similar to those in mice[33]. Nevertheless, we wanted to confirm this route of glycine catabolism in mice as well (Figure S2C). We observed labeling in mice from infused U13C-glycine into liver lactate and the TCA cycle intermediates (succinate and malate) (Figure 2D, Figure S2D). The hepatic labeling of serine, lactate and TCA cycle intermediates from glycine is lost with SHIN2 treatment (Figure S2E). Thus, in both mice and rats, serine produced by reverse SHMT flux feeds, presumably via serine dehydratase and pyruvate, into the liver TCA cycle.

Reverse SHMT2 flux requires a 1C unit in the form of methylene-THF, and one source of methylene-THF is the glycine cleavage system. We infused U13C-glycine in both wild-type and liver GLDC knockout mice and measured liver serine labeling. Odd isotope labeling of serine (M+1 & M+3) occurs when unlabeled or M+2 labeled glycine condenses with M+1 labeled 1C unit made from glycine by the glycine cleavage system (Figure 2A). Such odd-labeled serine was readily observable in wildtype mice and accounted quantitatively (after correction for the extent of glycine labeling) for 17% of liver 1C units (Figure 2E, Figure S2F-G). As expected, such labeling was lost with GLDC knockout. Loss of the glycine cleavage system, however, did not alter serine M+2 labeling from infused U13C-glycine, reflecting the sufficiency of other sources of methylene-THF to drive reverse SHMT2 flux (Figure 2E). Thus, glycine clearance by reverse SHMT2 flux can occur independent of glycine cleavage system activity.

Glycine- and serine-deficient diets decrease circulating levels selectively in fed state

In mammals, circulating serine and glycine comes from three sources: (i) dietary protein catabolism, (ii) endogenous protein breakdown, or (iii) de novo serine synthesis from the glycolytic intermediate 3-phosphoglycerate (Figure 3A). Serine- and glycine-free diets are well tolerated by mice for months and slow growth of some cancers[11,34,35]. Having uncovered an unexpected glycine homeostatic pathway (liver SHMT2 pathway), we turned to how serine and glycine homeostasis is maintained. To this end, we studied mice fed purified amino acid diets, where each amino acid is included in its free form in place of intact dietary protein to allow for the selective removal of individual amino acids (Figure 3A-B). It has previously been reported that serine-and glycine-free diets decrease circulating levels of both amino acids by about 50%, which we also observed to be true in the fed state (Figure 3C)[34]. Interestingly, however, we observed no change in fasted mice (Figure 3C). Indeed, for mice on the ser/gly-free diet, serine and glycine levels were higher in the fasted than the fed state, presumably reflecting endogenous protein degradation being greater in fasted than fed animals (Figure 3C)[36-38]. Like circulating levels, tissue pools were depleted

in fed state and maintained in fasted state when mice consumed the ser/gly-free chow (Figure S3A-D). The minimalist interpretation is that the serine-and glycine-free diet is hardly altering fasted serine or glycine metabolism (de novo synthesis from glucose or from endogenous protein catabolism, or catabolism of either amino acid). Instead, the ser/gly-free diet is simply decreasing the dietary influx of these amino acids in the fed state from the chow. Indeed, we observed similar fasted circulatory fluxes (endogenous production rates) for both serine (no change) and glycine (modest decrease) across fasted mice on regular or serine-and glycine-free diet (Figure 3D).

To explore the flux from endogenous (non-dietary) protein catabolism to serine and glycine, we infused fasted mice with $13C_1$-valine, $13C_1$-phenylalanine, U13C-glycine or U13C-serine to calculate circulatory fluxes (F_{circ}) for each amino acid. Because valine and phenylalanine are essential amino acids, their fasted production is from endogenous protein catabolism[33,36,39]:

$$F_{circ,\ val\ \ fasted} = F_{val \leftarrow endogenous\ \ protein} \quad [1]$$

Protein catabolism generates all amino acids in proportion to their abundance in that protein. For serine, this implies

$$F_{ser \leftarrow endogenous\ \ protein} = F_{val \leftarrow endgenous\ \ protein} \bullet \frac{\text{Protein fraction}_{\text{Ser}}}{\text{Protein fraction}_{\text{Val}}} \quad [2]$$

and similarly for glycine (in place of serine) and phenylalanine (in place of valine). The protein fraction of serine (0.081), glycine (0.074), valine (0.068), and phenylalanine (0.040) was estimated based on codon frequency of each amino acid[40]. By comparing these production fluxes from endogenous protein catabolism to overall circulatory flux, we found that, in the fasted state, 60-90% of both serine and glycine production is from protein degradation on both control and ser/gly-free diet (Figure 3F-G). Pulse-chase of [U-^{13}C]serine further supported similar serine production from endogenous protein catabolism in both diets (Figure S3D). Consequently, protein degradation rather than de novo synthesis is the major source of whole-body production of these amino acids in fasted mice.

Loss of dietary source has minimal effect on endogenous production

Serine- and glycine-free diet selectively alters circulating serine and glycine levels in the fed state (Figure 3C). Consistent with this, we observed about 25% higher fed-state fluxes for both amino acids in mice receiving a full assortment of dietary amino acids, as opposed to a serine-and glycine-free diet (Figure 4A). We calculated flux from uptake of incoming dietary amino acids based on quantity of free serine and glycine contained in chow and total quantity of chow each mouse consumed per day (Figure S4A-B). Strikingly, after subtracting out incoming flux from diet, the remaining flux was unaltered on serine- and glycine-free diet (Figure 4B). This further supports endogenous production (de novo

synthesis and endogenous protein catabolism) being largely unaltered by dietary serine and glycine removal.

To probe more explicitly de novo serine synthesis, we used U13C-glucose tracing to measure contribution to total serine production flux. The fractional fed-state labeling of circulating serine from U13C-glucose tracer was increased in mice receiving serine-and glycine-free diet (Figure 4C). This increase, however, could potentially simply reflect less dilution from dietary serine, as opposed to higher de novo synthesis. Indeed, multiplying the fraction of circulating serine coming from glucose by the serine circulatory turnover flux, to quantify the de novo synthetic flux, revealed no change between normal and serine-and glycine-free diet (Figure 4D, Figure S4C). Through infusion also of labeled threonine, we fully quantified known serine and glycine synthetic routes, each of which contributed substantially and together accounted fully (control diet) or nearly fully (85% serine- and glycine-free diet) for observed serine and glycine fluxes, with the missing 15% potentially reflecting an unmeasured source or experimental error (Figure 4E-F).

The unchanged de novo production of serine and glycine when these amino acids are removed from the diet was striking. We wondered if this might reflect the lack of specific mechanisms for sensing dietary serine, with physiological sensing instead focused on overall dietary protein. Feeding a low-protein diet (5%), however, similarly did not alter de novo serine synthetic flux, despite moderately increased phosphorylated eIF2a levels in liver indicating activation of integrated stress response (Figure 4C-D, Figure S4C-E)[41]. Overall, across the three dietary conditions in both fed and fasted states, we observed a trend toward higher serine synthesis from circulating U13C-glucose in the fed state, resulting in a correlation between circulating glucose flux and serine biosynthetic flux (Figure 4G). This may reflect in part higher 3-phosphoglycerate labeling from circulating glucose in fed mice. Most importantly, we observed no relationship between circulating serine levels and de novo synthesis flux from glucose (Figure 4H), implying the lack of a dedicated homeostatic mechanism in mouse to turn on endogenous serine synthesis when circulating serine is depleted.

Homeostasis is maintained by modulating serine and glycine consumption

Since overall circulatory turnover fluxes of glycine and serine are decreased on the serine- and glycine-deficient diet, consumption of these amino acids must also be decreased to maintain steady-state circulating levels (Figure 4A). A number of circulating metabolites, including some amino acids, are cleared by TCA cycle oxidation driven by mass action[36]. We hypothesized that suppressed circulating levels of serine and glycine, induced by the dietary deficiency, leads to decreased catabolism by the SHMT2-serine dehydratase-TCA cycle pathway. To test this, we measured liver labeling of TCA cycle intermediates from U13C-glycine and U13C-serine infusions on control or ser/gly-free diets. The malate fractional labeling from both U13C-glycine and U13C-serine was decreased in mice on the deficient diet (Figure 5A, Figure S5A-B), which is consistent with mass action clearance for both glycine and serine. Further supporting clearance by mass action, liver malate labeling from U13C-glycine correlates linearly with glycine concentration across its physiological concentration range (Figure 5B). This flux from glycine into the TCA cycle depends on

SHMT catalytic activity, as it is ablated by SHIN2 treatment (Figure 5B). Thus, de novo synthesis from glucose is constant, and homeostasis in response to altered dietary serine and glycine instead requires variable clearance by TCA cycle oxidation (Figure 5C).

Elevating glycine by hepatic SHMT2 loss fails to improve diet-induced hepatic steatosis

A common hallmark of metabolic syndrome is decreased glycine levels. We were accordingly curious whether reversing this glycine depletion by hepatic SHMT2 deletion would impact diet-induced hepatic steatosis in mice[42]. Consistent with previous reports, C57BL/6 mice placed on a Western Chow diet (Envigo TD.88137, 42% fat with sucrose) for 12 weeks had decreased circulating glycine levels with increased body weight, liver weight and liver triglyceride levels compared to mice on standard chow (PicoLab Rodent 20 5053) (Figure 6A, Figure S6A-D)[43]. To test whether restoring glycine levels would impact body weight, liver weight, or liver triglycerides, male and female *Shmt2*$^{flox/flox}$ mice were administered control (AAV8-TBG-Null) or Cre-expressing (AAV8-TBG-Cre) viral particles to induce SHMT2 liver knockout. The mice were then placed on Western diet for 12 weeks (Figure 6B). Loss of liver SHMT2 elevated circulating glycine levels also in mice fed Western diet, restoring them to slightly above levels of chow-fed wildtype mice (Figure 6C, Figure S6E-F). These SHMT2 liver KO mice, however, showed no difference in body weight, liver weight or liver triglyceride levels compared to Western diet-fed wildtype animals (Figure 6D-F). Thus, diet-induced obesity and fatty liver are not reversed by restoration of glycine levels via specific hepatic SHMT2 blockade. This contrasts with evidence that glycine supplementation can ameliorate hepatic steatosis[43,44], perhaps reflecting such supplementation impacting liver fat via mechanisms that require intact SHMT2.

DISCUSSION

This study finds that a primary route of mammalian glycine clearance is hepatic conversion to serine via reverse SHMT2 flux. This reverse flux through liver SHMT2 occurs in proportion to substrate levels, following mass action and thereby facilitating glycine homeostasis without substantial changes in biosynthetic flux.

All chemical reactions can occur in both the forward and reverse directions. The laws of thermodynamics dictate that net flux is in the direction with a negative Gibbs free energy change[45]. In metabolism, compartmentalization enables different reaction direction across organelles, cell types, or tissues. Glucose consumption by muscle glycolysis and production by hepatic gluconeogenesis is a classic example of opposite flux directions across tissues. Here we show the direction of SHMT flux is similarly tissue-dependent. Reverse SHMT2 flux in the liver occurs in concert with 1C-unit generating forward flux in proliferative cells like activated T cells. Such 1C-generating flux is of great physiological importance, but apparently lesser in absolute magnitude than SHMT2-mediated liver glycine consumption.

There is evidence of this net reverse SHMT1/2 flux in humans. Healthy and obese volunteers were infused with [U13C]glycine and [2,3,3-2H3]serine tracers to explore the impact of obesity on glycine metabolism[46]. While this work focused on flux differences between the two group and did not discuss the potential for whole-body SHMT flux to be

net glycine consuming, the authors report quantitative fluxes from serine to glycine, and vice versa. Notably, the greater flux, by about two-fold (123 μmol/kg lean body mass/h), is in the glycine-consuming direction.

Both SHMT2 and GCS clear hepatic glycine within mitochondria. It is feasible that these reactions together form a single clearance pathway consuming two glycine molecules by using the 1C unit from GCS as a substrate for SHMT2[47]. We find, however, that GCS loss does not block hepatic serine labeling from U13C-glycine. Moreover, U13C-glycine infusions in humans show that GCS provides less than half of the 1C units consumed by reverse SHMT flux[46,48]. Other sources of mitochondrial 1C units in liver include choline and betaine.

In cancer cell lines, removal of serine and glycine from culture media increases de novo synthesis from glucose[5,11,49]. This occurs by some combination of increased glycolytic carbon supply due to allosteric suppression of PKM2 activity and transcriptional activation of serine synthesis pathway genes by activating transcription factor 4 (ATF4)[5,10,50]. In vivo, however, we observed no induction of de novo serine or glycine synthesis in response to removal of these nonessential amino acids from the diet. One interpretation is that serine and glycine levels do not fall low enough to lead to uncharged tRNA and ATF4 induction. In an effort to trigger such responses, we also examined mice on a low protein (5%) diet, where insufficiency of essential amino acids has been reported to activate, via uncharged tRNA, integrated stress response kinase GCN2 leading to ATF4 expression, but again we did not observe increased de novo serine or glycine synthesis[51].

Consistent with endogenous serine and glycine metabolism remaining largely unaltered in response to diets lacking these amino acids, even the levels of serine and glycine stay the same except after eating, when they are lower due to lack of dietary influx. These observations are particularly important as serine and glycine-free diets have anticancer activity in mice and are currently being tested in humans (NCT05183295)[11,34,35,52-55]. Our data suggest that the impact of these diets, at least in mice, is limited to the fed state.

Given that production fluxes do not change, how is homeostasis maintained in response to serine and glycine-free diet? The simplest possibility is suppressed mass action-mediated consumption. Elevated levels of many metabolites lead, in linear proportion, to their enhanced consumption[36]. Here we find that suppressed serine and glycine levels, due to the dietary absence, lead in linear proportion to suppressed consumption. These data thus further support mass action as a central homeostatic mechanism in mammalian metabolism.

Proper glycine homeostasis is strongly associated with metabolic health. Humans with obesity, type II diabetes and non-alcoholic fatty liver disease have modestly decreased circulating glycine concentrations (down 10-20%)[42]. More generally, glycine level has an inverse association with BMI and weight loss interventions consistently increase glycine, tending to restore healthy levels[46,56,57]. Despite systematic studies in both rodents and patients, it remains unclear if impaired de novo synthesis or elevated catabolism drives this glycine depletion[43,58,59]. Studies on glycine catabolism in metabolic syndrome have focused on GCS flux. GCS flux was unchanged in fatty liver disease patients compared to

healthy individuals[60]. Our work here uncovers glycine consumption by SHMT2. Blocking this consumption route in mice by liver SHMT2 loss did not improve development of hepatic steatosis. This does not preclude potential benefits on other aspects of metabolic syndrome. Further investigation of whether this pathway is enhanced in metabolic syndrome to cause decreased glycine levels and whether such modulation of the pathway contributes to downstream sequelae of fatty liver, including fibrosis, merits exploration.

Limitations of Study

A limitation of this investigation is the use of purified diets to selectively manipulate amino acid availability. Under normal conditions, dietary protein is consumed and the intact protein must be absorbed and degraded to produce free amino acids. The mice consuming a purified diet were in an atypical physiological state where free amino acids were directly absorbed, bypassing the need for dietary protein degradation. It has been shown that free amino acids are more rapidly absorbed than intact protein, leading to increased amino acid levels in circulation and changes in gut microbiome metabolism[61]. Methodologically, we also carried out amino acid tracer infusions, which reached up to 20% labeling enrichment in circulation. Such infusions provide an additional (albeit modest) amino acid source, which could potentially alter endogenous metabolism, in settings such as fasting. Further, healthy mice were used for this study and placed on the ser/gly-free diet for three weeks. Homeostatic changes in glycine and serine production or consumption that occur after longer time on the deficient diet were not explored. Work was also limited to rodents. Other mechanisms of serine and glycine homeostasis may exist in other mammals including humans.

STAR METHODS

RESOURCE AVAILABILITY

LEAD CONTACT

Further information and requests for resources and reagents should be directed to and will be fulfilled by the Lead Contact, Joshua D. Rabinowitz (joshr@princeton.edu).

MATERIALS AVAILABILITY

The *Shmt2*$^{flox/flox}$ mouse strain was generated as part of this study and is available upon request.

DATA AND CODE AVAILABILITY

El-Maven (Elucidata) and AccuCor Isotope Natural Abundance Correction used for the analysis of LC-MS data is available on GitHub (https://github.com/lparsons/accucor). Metabolomics and isotope labeling data generated during this study is included as Data S1. Metabolomics data have been deposited at the National Metabolomics Data Repository with Study ID: ST002980.

EXPERIMENTAL MODEL AND SUBJECT DETAILS

Mouse and rat studies followed protocols approved by the Animal Care and Use Committee for Princeton University. C57BL/6N mice were obtained from Charles River Laboratories. *Shmt2*$^{flox/flox}$ mice in the C57BL/6 background were generated by Genome Editing Shared Resource at Rutgers University, and bred at Princeton University. *Shmt1*$^{KO/KO}$ mice were a generous gift from P.J. Stover and bred at Princeton University. *Gldc*$^{flox/flox}$ mice in the C57BL/6NJ background were obtained from Jackson Laboratory (strain #: 034928) and bred at Princeton University. Mice were allowed at least 5 days of acclimation to the facilities prior to experimentation, were randomly chosen for experimental groups and were on a normal light cycle (8 AM – 8 PM). Mouse experiments were performed on 10-14 week old animals. Animals received either a normal chow diet (PicoLab Rodent 20 5053 laboratory Diet St. Louis, MO) or an amino acid purified diet from TestDiet: Control (5WTV), serine and glycine-free (5B62), or low protein (5Z7D). Control and serine/glycine-free diets provide energy 15% from protein (as free amino acids), 17% from fat and 68% from carbohydrates. All amino acids were elevated proportionally to maintain total protein level in serine/glycine-free diet. Low protein diet provides energy 5% from protein (as free amino acids), 17% from fat and 78% from carbohydrates. Animals received purified diets 21 days prior to experimentation. For rat experiments, Sprague Dawley rats with arterial and jugular vein catheters were obtained at 5 weeks of age from Charles River Laboratory, received normal chow diet (PicoLab Rodent 20 5053 laboratory Diet St. Louis, MO) and acclimated to environment and human handling for 3 weeks prior to experiments.

METHOD DETAILS

Serum collection and tissue harvesting—Fasted samples were collected from mice 8 hours after food removal (chow removed at 9AM and sample collected at 5PM). Ad lib fed samples were collected at 8AM. Tail blood was collected in live mice by tail snip. Blood was directly collected into blood collection tubes with clotting factor (Sarstedt 16.442.100). Blood samples were stored on ice and then centrifuged at 16,000 x g for 10 min at 4°C to collect serum (top layer). Tissue harvest was performed after euthanasia by cervical dislocation. Tissues were quickly dissected in the order of liver, spleen, pancreas, kidney, small intestine, quadricep, diaphragm, heart, lung, brain and ears (skin). Tissues were clamped with a pre-cooled Wollenberger clamp in tin foil, and dropped in liquid nitrogen. Serum and tissue samples were stored at −80°C.

Stable isotope infusions in mice—Aseptic surgery was performed to place a catheter in the right jugular vein and to connect the catheter to a vascular access button implanted under the skin on the back of the mouse. Catheters and vascular access buttons (VABs) were bought from Instech Labs. Mice were allowed to recover from jugular vein catheterization surgery for at least 5 days before experimentation. For intravenous infusions, 13C-metabolites (Cambridge Isotope Laboratories) were prepared in saline at following concentrations: 0.2 M (fasted) and 0.8 M (fed) U-13C-glucose (CLM-1396), 40 mM U-13C-glycine (CLM-1017), 30 mM U-13C-serine (CLM-1574), 5 mM $13C_1$-valine (CLM-470), and 5 mM $13C_1$-phenylalanine (CLM-762). The infusion setup (Instech Laboratories) included a swivel and tether to allow the mouse to move around the cage freely. Infusion rate was set to 0.1 μL/min/g body weight and tracer infused for 150 minutes followed by tail

blood collection and tissue harvesting. Fasted infusions were collected at 5PM 8 hours after chow removal (started infusion at 2:30PM). Re-fed infusions were in mice fasted at 9AM, chow replaced and infusion started at 8PM, and infusion completed at 10:30PM.

Stable isotope infusions in rats with arterial and venous blood collection—Chow was removed at 9AM and infusion finished at 5PM. 40 mM U-13C-glycine (CLM-1017) and 50 mM U-13C-serine (CLM-1574) was prepared in saline and infused at a rate of 0.1 μL/min/g body weight for 5 hours. Arterial blood was collected via catheter, and then the animal was anesthetized by pentobarbital administered through jugular vein catheter (55 mg/kg priming dose over one minute followed by 2.3 mg/kg/hr maintenance dose). After 20 minutes, rat was surgically opened and blood from renal, hepatic, portal and tail veins was collected using a syringe. Blood samples were placed on ice and centrifuged at 16,000 x g for 10 min at 4°C for serum collection.

Pharmacological SHMT1/2 inhibition—The small molecule SHMT inhibitor SHIN2 was dissolved in 20% 2-hydroxypropyl-β-cyclodextrin as a 20 mg/ml stock and diluted in 0.9% saline to the desired concentration. Drug or vehicle control was intravenously infused through the jugular vein catheter at an infusion rate of 16.7 mg/kg/hr, which is equivalent to 200 mg/kg SHIN2 over a 12-hour period.

Liver-specific gene knockout—*Shmt2*$^{flox/flox}$ mice or *Gldc*$^{flox/flox}$ mice along with wildtype litter mate controls were administered 2x10^{11} genomic copies of AAV8-*TBG*-Cre viral particles (Addgene, #107787) by tail vein injection (100 μL of 2x10^{12} genomic copies per mL stock). Experiments were carried out 21 days after virus injection.

Diet-induced hepatic steatosis—*Shmt2*$^{flox/flox}$ mice were administered 2x10^{11} genomic copies of AAV8-*TBG*-Cre viral particles (Addgene, #107787) or AAV8-TBG-Null (Addgene, #105536) by tail vein injection (100 μL of 2x10^{12} genomic copies per mL stock) and placed on Western Diet (Envigo TD.88137, 42% fat with sucrose) for 12 weeks. Liver triglyceride levels were quantified by Triglyceride-Glo Assay kit (J3160, Promega).

Immunoblot analysis—Protein lysates were prepared from liver samples by 2% SDS whole cell lysis and sonication and quantified by BCA assay. Standard protocols were used for the detection of proteins by immunoblot (IB) analysis and the primary antibodies used are Shmt2 (CST, E7F4Q), Gldc (CST, 12794), Actin (CST, E4DZ9), eILF2a (CST, 9722), and phospho-eILF2a (CST, 3597). Membranes were developed using IRDye (LI-COR Biosciences) secondary antibodies for visualization and density quantification by the LI-COR Odyssey Imaging System (LI-COR Biosciences).

Metabolite extraction of serum—Serum (3 μl) was extracted with cold 100% methanol (40X), vortexed, and cooled on wet ice for ten minutes. For absolute quantification, a standard mix of N15-isotope labeled serine (51 μM) and glycine (206 μM) was spiked-in at equal volume to the serum sample (3 μl). Then, the extract was centrifuged at 16,000 x g for 10 minutes at 4°C and supernatant was transferred to tubes for LC-MS analysis.

Metabolite extraction of tissues—Frozen tissue pieces were pulverized using a Cryomill (Retsch) at cryogenic temperature. Ground tissue was weighed (10–20 mg) and transferred into a precooled tube for extraction. Soluble metabolites extraction was done by adding −20 °C 40:40:20 methanol:acetonitrile:water with 1 mM N-ethylmaleimide (for alkylation of thiol containing metabolites) to the resulting powder (40 µl solvent per mg tissue) [62]. For absolute quantification, a standard mix of isotope labeled metabolites of known concentration was spiked-in at a volume of 1 µl per mg tissue. Samples were vortexed for 10 seconds, cooled at 4°C (on wet ice) for 10 minutes and then centrifuged at 4 °C at 16,000 x *g* for 30 minutes. Supernatant was transferred to LC–MS vials for analysis.

Metabolite measurement by LC-MS—LC–MS analysis for soluble metabolites was achieved on a quadrupole-orbitrap mass spectrometer (Thermo Scientific): the Q Exactive PLUS hybrid, Exploris 240 or Exploris 480. Each mass spectrometer was coupled to hydrophilic interaction chromatography (HILIC) via electrospray ionization. To perform the LC separation of serum and tissue samples, an XBridge BEH Amide column (150 mm × 2.1 mm, 2.5 µM particle size, Waters) was used with a gradient of solvent A (95%:5% H2O: acetonitrile with 20 mM ammonium acetate, 20 mM ammonium hydroxide, pH 9.4), and solvent B (100% acetonitrile). The gradient was 0 minutes, 85% B; 2 minutes, 85% B; 3 minutes, 80% B; 5 minutes, 80% B; 6 minutes, 75% B; 7 minutes, 75% B; 8 minutes, 70% B; 9 minutes, 70% B; 10 minutes, 50% B; 12 minutes, 50% B; 13 minutes, 25% B; 16 minutes, 25% B; 18 minutes, 0% B; 23 minutes, 0% B; 24 minutes, 85% B; 30 minutes, 85% B. The flow rate was 150 µl min^{-1}, an injection volume of 10 µl for serum samples and 5 µl for tissue samples, and column temperature was 25°C. MS full scans were in negative or positive ion mode with a resolution of 140,000 at *m/z* 200 and scan range of 70–1,000 *m/z*. The automatic gain control (AGC) target was 1×10^6. LC-MS peak files were analyzed and visualized with El-MAVEN (Elucidata) using 5 ppm ion extraction window, minimum peak intensity of 1 x 10^5 ions, and minimum signal to background blank ratio of 2. For infusion experiments, the software package Accucor was used to correct for metabolite labeling from natural isotope abundance[63].

Definition of normalized metabolite labeling—When the 13C-labeled tracer X is infused, the normalized labeling of downstream metabolite Y is defined as L_Y / L_X, where L_X and L_Y are the fraction of labeled carbon atoms for metabolite X and Y defined as

$$L = \frac{i \bullet \sum_{i=0}^{C} L_{[M+i]}}{C} \quad [3]$$

where $L_{[M+i]}$ is the fraction of mass isotopomer [M + i] and C is the total number of carbons in the metabolite. For infusions in mice, L_X is the steady-state labeling in serum and L_Y is the labeling in serum or tissues. For infusions in rats, L_X is the labeling of blood into the liver (calculated based on 22% of arterial blood labeling and 78% portal vein blood labeling as shown in Equation 4, both of which were directly measured) and L_Y is the labeling of the blood draining from the liver (hepatic vein)[32].

$$L_{Liver\ \ blood\ \ supply,lactate} = (0.22 \bullet L_{artery,lactate}) + (0.78 \bullet L_{portal,lactate})$$

[4]

Quantifying net production/consumption fluxes—The net serine and glycine tissue fluxes in rats were calculated using the following equation

$$J_{net} = Q(C_v - C_a)$$

[5]

where Q is the cardiac output for the draining vein (Q_{portal} = 0.153, $Q_{hepatic}$ = 0.183, Q_{renal} = 0.141 mL/min/g Rat) and C_v is the measured serine or glycine concentration in the draining vein and C_a is the concentration in the incoming blood supply (artery for portal and renal and 22% artery and 78% portal vein for hepatic)[43,44].

Circulating turnover flux measurements—To measure the circulating (whole-body) turnover flux of a metabolite, we infused U13C-labeled form of the metabolite. At pseudo-steady state, we measured the mass isotope distribution of the metabolite in serum and the intact tracer circulatory turnover flux (F_{circ}) was calculated as previously described. The fraction of the fully labeled tracer (i.e., the infused form), L_{M+C} (for example, glycine is M+2 due to having two carbon atoms) was used:

$$F_{circ} = R \bullet \frac{1 - L_{[M+C]}}{L_{[M+C]}}$$

[6]

where R is the infusion rate of the labeled tracer. Since the turnover flux is a pseudo-steady state measurement, for minimally perturbative tracer infusions, production flux is approximately equal to consumption flux of the metabolite and thus F_{circ} reflects both the circulating production and consumption fluxes of the infused metabolite.

Contribution of non-essential amino acid production flux from protein degradation—Turnover flux of the essential amino acid valine was used to quantify production from endogenous protein catabolism of the non-essential amino acids serine and glycine in the fasted state, as defined in equations [1] and [2]. Valine is an essential amino acid in mammals due to the absence of biosynthetic enzymes that permit the transformation of other dietary nutrients, such as glucose, into the amino acid valine. Consequently, valine comes either from the diet or endogenous protein degradation. In the control and ser/gly-free experimental conditions, we use a purified diet where each amino acid is added to the diet in the free form (diet contains no intact protein) and thus these mice obtain free valine directly from consuming the purified chow. When we fast the mice to obtain fasted F_{circ} measurements, the mice are placed in new cages without food for a total of 8 hours prior to the completion of the infusion experiment. F_{circ} is a measure of whole-body production and so in these fasted mice, the valine F_{circ} is the rate of valine production that is coming

from a non-dietary source (since the mice no longer have access to chow, for 8 h, which is long enough for food to clear the mouse intestine). Since valine is produced from protein catabolism, the non-dietary source of valine is degradation of endogenous protein. Consequently, as shown in Equation 1, valine F_{circ} in fasted mice, when no dietary source is present, is a measurement of valine production from endogenous protein catabolism.

Relative frequency (molar fraction) of valine (0.068), serine (0.081) and glycine (0.074) in protein was estimated for this analysis based on observed codon frequency in vertebrates[40]. While contribution of an individual protein to the production of free amino acids will vary from one protein to the next, this approximation actually reflects the overall amino acid outflow from whole body protein, as confirmed by its accurately predicting relative fasted-state production (F_{circ}) of different essential amino acids[33,39]. Protein degradation flux is decreased in the fed state and amino acid production fluxes from protein degradation were taken to be 49% of fasted state fluxes based on prior literature data[36].

Contribution of diet to amino acid production flux—Since amino acid purified chow have a defined quantity of serine and glycine, the proportion of turnover flux from diet in the fed state was calculated from quantity of chow consumed. The control chow (TestDiet, 5WTV) was 1.0% serine and 0.9% glycine by weight, so assuming 100% of amino acids consumed in chow reaches circulation, the production flux from diet ($F_{AA \leftarrow diet}$) is calculated by

$$F_{AA<-diet} = R_{chow\ consumed} \bullet Abn_{AA\ in\ diet} \quad [7]$$

where $R_{chow\ consumed}$ is quantity of chow eaten by the mice per hour and $Abn_{AA\ in\ diet}$ is the abundance of the amino acid within the diet. All other production flux comes from endogenous sources, so endogenous production flux ($F_{AA \leftarrow endogenous}$) is calculated by

$$F_{AA<-endogenous} = F_{circ} - F_{AA<-diet} \quad [8]$$

De novo serine synthesis flux from circulating glucose—To measure the flux of serine carbons synthesized from circulating glucose, we performed U13C-glucose infusions and measured the normalized carbon labeling of serine in serum ($L_{ser \leftarrow glucose}$). From this, the flux of serine produced from glucose is calculated by

$$F_{ser<-glucose} = F_{circ,\ ser} \bullet L_{ser<-glucose} \quad [9]$$

QUANTIFICATION AND STATISTICAL ANALYSIS

Data are presented as means with error bars representing the standard error of the mean. A two-sided t-test was used to calculate p values and a p value of less than 0.05 was considered significant (*<0.05, **<0.01, ***<0.001, <0.0001). For metabolomics, p value

was corrected for multiple comparisons with a false discovery rate (FDR) cutoff of 0.1. Prism (GraphPad) was used for statistical analysis.

Supplementary Material

Refer to Web version on PubMed Central for supplementary material.

ACKNOWLEDGEMENTS

M.J.M is funded by NIH grant F32CA250190. This work was funded by NIH Pioneer award DP1DK113643, SU2C Convergence Award 3.1416, and Ludwig Cancer Research to J.D.R. We are grateful to members of the Rabinowitz group for scientific discussions and insights. Illustrations prepared with assistance from biorender.com.

REFERENCES

1. Gao X, Lee K, Reid MA, Sanderson SM, Qiu C, Li S, Liu J, and Locasale JW (2018). Serine Availability Influences Mitochondrial Dynamics and Function through Lipid Metabolism. Cell Rep 22, 3507–3520. 10.1016/j.celrep.2018.03.017. [PubMed: 29590619]
2. Bröer S, and Bröer A (2017). Amino acid homeostasis and signalling in mammalian cells and organisms. Biochem J 474, 1935–1963. 10.1042/bcj20160822. [PubMed: 28546457]
3. Gaggini M, Carli F, Rosso C, Buzzigoli E, Marietti M, Della Latta V, Ciociaro D, Abate ML, Gambino R, Cassader M, et al. (2018). Altered amino acid concentrations in NAFLD: Impact of obesity and insulin resistance. Hepatology 67, 145–158. 10.1002/hep.29465. [PubMed: 28802074]
4. Guasch-Ferré M, Hruby A, Toledo E, Clish CB, Martínez-González MA, Salas-Salvadó J, and Hu FB (2016). Metabolomics in Prediabetes and Diabetes: A Systematic Review and Meta-analysis. Diabetes Care 39, 833–846. 10.2337/dc15-2251. [PubMed: 27208380]
5. Chaneton B, Hillmann P, Zheng L, Martin ACL, Maddocks ODK, Chokkathukalam A, Coyle JE, Jankevics A, Holding FP, Vousden KH, et al. (2012). Serine is a natural ligand and allosteric activator of pyruvate kinase M2. Nature 491, 458–462. 10.1038/nature11540. [PubMed: 23064226]
6. Fell DA, and Snell K (1988). Control analysis of mammalian serine biosynthesis. Feedback inhibition on the final step. Biochem J 256, 97–101. 10.1042/bj2560097. [PubMed: 2851987]
7. Snell K. (1984). Enzymes of serine metabolism in normal, developing and neoplastic rat tissues. Adv Enzyme Regul 22, 325–400. 10.1016/0065-2571(84)90021-9. [PubMed: 6089514]
8. Ducker GS, Chen L, Morscher RJ, Ghergurovich JM, Esposito M, Teng X, Kang Y, and Rabinowitz JD (2016). Reversal of Cytosolic One-Carbon Flux Compensates for Loss of the Mitochondrial Folate Pathway. Cell Metab 23, 1140–1153. 10.1016/j.cmet.2016.04.016. [PubMed: 27211901]
9. Edgar AJ (2002). The human L-threonine 3-dehydrogenase gene is an expressed pseudogene. BMC Genet 3, 18. 10.1186/1471-2156-3-18. [PubMed: 12361482]
10. Ye J, Mancuso A, Tong X, Ward PS, Fan J, Rabinowitz JD, and Thompson CB (2012). Pyruvate kinase M2 promotes de novo serine synthesis to sustain mTORC1 activity and cell proliferation. Proc Natl Acad Sci U S A 109, 6904–6909. 10.1073/pnas.1204176109. [PubMed: 22509023]
11. Maddocks OD, Berkers CR, Mason SM, Zheng L, Blyth K, Gottlieb E, and Vousden KH (2013). Serine starvation induces stress and p53-dependent metabolic remodelling in cancer cells. Nature 493, 542–546. 10.1038/nature11743. [PubMed: 23242140]
12. Yang M, and Vousden KH (2016). Serine and one-carbon metabolism in cancer. Nat Rev Cancer 16, 650–662. 10.1038/nrc.2016.81. [PubMed: 27634448]
13. Locasale JW (2013). Serine, glycine and one-carbon units: cancer metabolism in full circle. Nat Rev Cancer 13, 572–583. 10.1038/nrc3557. [PubMed: 23822983]
14. Meiser J, Tumanov S, Maddocks O, Labuschagne CF, Athineos D, Van Den Broek N, Mackay GM, Gottlieb E, Blyth K, Vousden K, et al. (2016). Serine one-carbon catabolism with formate overflow. Sci Adv 2, e1601273. 10.1126/sciadv.1601273. [PubMed: 27819051]
15. Ducker GS, and Rabinowitz JD (2017). One-Carbon Metabolism in Health and Disease. Cell Metab 25, 27–42. 10.1016/j.cmet.2016.08.009. [PubMed: 27641100]

16. Tani H, Ohnishi S, Shitara H, Mito T, Yamaguchi M, Yonekawa H, Hashizume O, Ishikawa K, Nakada K, and Hayashi JI (2018). Mice deficient in the Shmt2 gene have mitochondrial respiration defects and are embryonic lethal. Sci Rep 8, 425. 10.1038/s41598-017-18828-3. [PubMed: 29323231]

17. Pai YJ, Leung KY, Savery D, Hutchin T, Prunty H, Heales S, Brosnan ME, Brosnan JT, Copp AJ, and Greene ND (2015). Glycine decarboxylase deficiency causes neural tube defects and features of non-ketotic hyperglycinemia in mice. Nat Commun 6, 6388. 10.1038/ncomms7388. [PubMed: 25736695]

18. Lee GY, Haverty PM, Li L, Kljavin NM, Bourgon R, Lee J, Stern H, Modrusan Z, Seshagiri S, Zhang Z, et al. (2014). Comparative oncogenomics identifies PSMB4 and SHMT2 as potential cancer driver genes. Cancer Res 74, 3114–3126. 10.1158/0008-5472.Can-13-2683. [PubMed: 24755469]

19. Ron-Harel N, Santos D, Ghergurovich JM, Sage PT, Reddy A, Lovitch SB, Dephoure N, Satterstrom FK, Sheffer M, Spinelli JB, et al. (2016). Mitochondrial Biogenesis and Proteome Remodeling Promote One-Carbon Metabolism for T Cell Activation. Cell Metab 24, 104–117. 10.1016/j.cmet.2016.06.007. [PubMed: 27411012]

20. Xue HH, Fujie M, Sakaguchi T, Oda T, Ogawa H, Kneer NM, Lardy HA, and Ichiyama A (1999). Flux of the L-serine metabolism in rat liver. The predominant contribution of serine dehydratase. J Biol Chem 274, 16020–16027. 10.1074/jbc.274.23.16020. [PubMed: 10347151]

21. Kikuchi G, Motokawa Y, Yoshida T, and Hiraga K (2008). Glycine cleavage system: reaction mechanism, physiological significance, and hyperglycinemia. Proc Jpn Acad Ser B Phys Biol Sci 84, 246–263. 10.2183/pjab.84.246.

22. Wang W, Wu Z, Dai Z, Yang Y, Wang J, and Wu G (2013). Glycine metabolism in animals and humans: implications for nutrition and health. Amino Acids 45, 463–477. 10.1007/s00726-013-1493-1. [PubMed: 23615880]

23. Van Hove JLK, Coughlin C II, Swanson M, and Hennermann JB (1993). Nonketotic Hyperglycinemia. In GeneReviews(®), Adam MP, Everman DB, Mirzaa GM, Pagon RA, Wallace SE, Bean LJH, Gripp KW, and Amemiya A, eds. (University of Washington, Seattle Copyright © 1993-2022, University of Washington, Seattle. GeneReviews is a registered trademark of the University of Washington, Seattle. All rights reserved.).

24. García-Cañaveras JC, Lancho O, Ducker GS, Ghergurovich JM, Xu X, da Silva-Diz V, Minuzzo S, Indraccolo S, Kim H, Herranz D, and Rabinowitz JD (2021). SHMT inhibition is effective and synergizes with methotrexate in T-cell acute lymphoblastic leukemia. Leukemia 35, 377–388. 10.1038/s41375-020-0845-6. [PubMed: 32382081]

25. Beaudin AE, Abarinov EV, Noden DM, Perry CA, Chu S, Stabler SP, Allen RH, and Stover PJ (2011). Shmt1 and de novo thymidylate biosynthesis underlie folate-responsive neural tube defects in mice. Am J Clin Nutr 93, 789–798. 10.3945/ajcn.110.002766. [PubMed: 21346092]

26. MacFarlane AJ, Liu X, Perry CA, Flodby P, Allen RH, Stabler SP, and Stover PJ (2008). Cytoplasmic serine hydroxymethyltransferase regulates the metabolic partitioning of methylenetetrahydrofolate but is not essential in mice. J Biol Chem 283, 25846–25853. 10.1074/jbc.M802671200. [PubMed: 18644786]

27. Kos CH (2004). Cre/loxP system for generating tissue-specific knockout mouse models. Nutr Rev 62, 243–246. 10.1301/nr2004.jun243-246. [PubMed: 15291397]

28. Leung KY, De Castro SCP, Santos C, Savery D, Prunty H, Gold-Diaz D, Bennett S, Heales S, Copp AJ, and Greene NDE (2020). Regulation of glycine metabolism by the glycine cleavage system and conjugation pathway in mouse models of non-ketotic hyperglycinemia. J Inherit Metab Dis 43, 1186–1198. 10.1002/jimd.12295. [PubMed: 32743799]

29. Handzlik MK, and Metallo CM (2023). Sources and Sinks of Serine in Nutrition, Health, and Disease. Annu Rev Nutr 43, 123–151. 10.1146/annurev-nutr-061021-022648. [PubMed: 37307855]

30. Hetenyi G Jr., Anderson PJ, Raman M, and Ferrarotto C (1988). Gluconeogenesis from glycine and serine in fasted normal and diabetic rats. Biochem J 253, 27–32. 10.1042/bj2530027. [PubMed: 3138983]

31. Rowsell EV, Carnie JA, Wahbi SD, Al-Tai AH, and Rowsell KV (1979). L-serine dehydratase and L-serine-pyruvate aminotransferase activities in different animal species. Comp Biochem Physiol B 63, 543–555. 10.1016/0305-0491(79)90061-0. [PubMed: 318433]
32. Eipel C, Abshagen K, and Vollmar B (2010). Regulation of hepatic blood flow: the hepatic arterial buffer response revisited. World J Gastroenterol 16, 6046–6057. 10.3748/wjg.v16.i48.6046. [PubMed: 21182219]
33. Hui S, Ghergurovich JM, Morscher RJ, Jang C, Teng X, Lu W, Esparza LA, Reya T, Le Z, Yanxiang Guo J, et al. (2017). Glucose feeds the TCA cycle via circulating lactate. Nature 551, 115–118. 10.1038/nature24057. [PubMed: 29045397]
34. Maddocks ODK, Athineos D, Cheung EC, Lee P, Zhang T, van den Broek NJF, Mackay GM, Labuschagne CF, Gay D, Kruiswijk F, et al. (2017). Modulating the therapeutic response of tumours to dietary serine and glycine starvation. Nature 544, 372–376. 10.1038/nature22056. [PubMed: 28425994]
35. Tajan M, Hennequart M, Cheung EC, Zani F, Hock AK, Legrave N, Maddocks ODK, Ridgway RA, Athineos D, Suárez-Bonnet A, et al. (2021). Serine synthesis pathway inhibition cooperates with dietary serine and glycine limitation for cancer therapy. Nat Commun 12, 366. 10.1038/s41467-020-20223-y. [PubMed: 33446657]
36. Li X, Hui S, Mirek ET, Jonsson WO, Anthony TG, Lee WD, Zeng X, Jang C, and Rabinowitz JD (2022). Circulating metabolite homeostasis achieved through mass action. Nat Metab 4, 141–152. 10.1038/s42255-021-00517-1. [PubMed: 35058631]
37. Grunnet N, and Dich J (1998). Effect of fasted and fed conditions of protein turnover in perfused cultured hepatocytes. Nutrition 14, 23–29. 10.1016/s0899-9007(97)00389-4. [PubMed: 9437678]
38. Sinturel F, Gerber A, Mauvoisin D, Wang J, Gatfield D, Stubblefield JJ, Green CB, Gachon F, and Schibler U (2017). Diurnal Oscillations in Liver Mass and Cell Size Accompany Ribosome Assembly Cycles. Cell 169, 651–663.e614. 10.1016/j.cell.2017.04.015. [PubMed: 28475894]
39. Neinast MD, Jang C, Hui S, Murashige DS, Chu Q, Morscher RJ, Li X, Zhan L, White E, Anthony TG, et al. (2019). Quantitative Analysis of the Whole-Body Metabolic Fate of Branched-Chain Amino Acids. Cell Metab 29, 417–429.e414. 10.1016/j.cmet.2018.10.013. [PubMed: 30449684]
40. Tsuji J, Nydza R, Wolcott E, Mannor E, Moran B, Hesson G, Arvidson T, Howe K, Hayes R, Ramirez M, and Way M (2010). The Frequencies of Amino Acids Encoded by Genomes that Utilize Standard and Nonstandard Genetic Codes. BIOS 81, 22–31, 10.
41. Pakos-Zebrucka K, Koryga I, Mnich K, Ljujic M, Samali A, and Gorman AM (2016). The integrated stress response. EMBO Rep 17, 1374–1395. 10.15252/embr.201642195. [PubMed: 27629041]
42. Alves A, Bassot A, Bulteau AL, Pirola L, and Morio B (2019). Glycine Metabolism and Its Alterations in Obesity and Metabolic Diseases. Nutrients 11. 10.3390/nu11061356.
43. Rom O, Liu Y, Liu Z, Zhao Y, Wu J, Ghrayeb A, Villacorta L, Fan Y, Chang L, Wang L, et al. (2020). Glycine-based treatment ameliorates NAFLD by modulating fatty acid oxidation, glutathione synthesis, and the gut microbiome. Sci Transl Med 12. 10.1126/scitranslmed.aaz2841.
44. Qu P, Rom O, Li K, Jia L, Gao X, Liu Z, Ding S, Zhao M, Wang H, Chen S, et al. (2023). DT-109 ameliorates nonalcoholic steatohepatitis in nonhuman primates. Cell Metab 35, 742–757.e710. 10.1016/j.cmet.2023.03.013. [PubMed: 37040763]
45. Noor E, Bar-Even A, Flamholz A, Reznik E, Liebermeister W, and Milo R (2014). Pathway thermodynamics highlights kinetic obstacles in central metabolism. PLoS Comput Biol 10, e1003483. 10.1371/journal.pcbi.1003483. [PubMed: 24586134]
46. Tan HC, Hsu JW, Tai ES, Chacko S, Wu V, Lee CF, Kovalik JP, and Jahoor F (2022). De Novo Glycine Synthesis Is Reduced in Adults With Morbid Obesity and Increases Following Bariatric Surgery. Front Endocrinol (Lausanne) 13, 900343. 10.3389/fendo.2022.900343. [PubMed: 35757406]
47. Kikuchi G. (1973). The glycine cleavage system: composition, reaction mechanism, and physiological significance. Mol Cell Biochem 1, 169–187. 10.1007/bf01659328. [PubMed: 4585091]
48. Lamers Y, Williamson J, Gilbert LR, Stacpoole PW, and Gregory JF 3rd (2007). Glycine turnover and decarboxylation rate quantified in healthy men and women using primed, constant infusions

of [1,2-(13)C2]glycine and [(2)H3]leucine. J Nutr 137, 2647–2652. 10.1093/jn/137.12.2647. [PubMed: 18029478]

49. Jain M, Nilsson R, Sharma S, Madhusudhan N, Kitami T, Souza AL, Kafri R, Kirschner MW, Clish CB, and Mootha VK (2012). Metabolite profiling identifies a key role for glycine in rapid cancer cell proliferation. Science 336, 1040–1044. 10.1126/science.1218595. [PubMed: 22628656]
50. DeNicola GM, Chen PH, Mullarky E, Sudderth JA, Hu Z, Wu D, Tang H, Xie Y, Asara JM, Huffman KE, et al. (2015). NRF2 regulates serine biosynthesis in non-small cell lung cancer. Nat Genet 47, 1475–1481. 10.1038/ng.3421. [PubMed: 26482881]
51. Laeger T, Henagan TM, Albarado DC, Redman LM, Bray GA, Noland RC, Münzberg H, Hutson SM, Gettys TW, Schwartz MW, and Morrison CD (2014). FGF21 is an endocrine signal of protein restriction. J Clin Invest 124, 3913–3922. 10.1172/jci74915. [PubMed: 25133427]
52. Tajan M, and Vousden KH (2020). Dietary Approaches to Cancer Therapy. Cancer Cell 37, 767–785. 10.1016/j.ccell.2020.04.005. [PubMed: 32413275]
53. Muthusamy T, Cordes T, Handzlik MK, You L, Lim EW, Gengatharan J, Pinto AFM, Badur MG, Kolar MJ, Wallace M, et al. (2020). Serine restriction alters sphingolipid diversity to constrain tumour growth. Nature 586, 790–795. 10.1038/s41586-020-2609-x. [PubMed: 32788725]
54. Falcone M, Uribe AH, Papalazarou V, Newman AC, Athineos D, Stevenson K, Sauvé CG, Gao Y, Kim JK, Del Latto M, et al. (2022). Sensitisation of cancer cells to radiotherapy by serine and glycine starvation. Br J Cancer 127, 1773–1786. 10.1038/s41416-022-01965-6. [PubMed: 36115879]
55. Taylor SR, Falcone JN, Cantley LC, and Goncalves MD (2022). Developing dietary interventions as therapy for cancer. Nat Rev Cancer 22, 452–466. 10.1038/s41568-022-00485-y. [PubMed: 35614234]
56. Kraus WE, Pieper CF, Huffman KM, Thompson DK, Kraus VB, Morey MC, Cohen HJ, Ravussin E, Redman LM, Bain JR, et al. (2016). Association of Plasma Small-Molecule Intermediate Metabolites With Age and Body Mass Index Across Six Diverse Study Populations. J Gerontol A Biol Sci Med Sci 71, 1507–1513. 10.1093/gerona/glw031. [PubMed: 26984390]
57. Lustgarten MS, Price LL, Phillips EM, and Fielding RA (2013). Serum glycine is associated with regional body fat and insulin resistance in functionally-limited older adults. PLoS One 8, e84034. 10.1371/journal.pone.0084034. [PubMed: 24391874]
58. White PJ, Lapworth AL, McGarrah RW, Kwee LC, Crown SB, Ilkayeva O, An J, Carson MW, Christopher BA, Ball JR, et al. (2020). Muscle-Liver Trafficking of BCAA-Derived Nitrogen Underlies Obesity-Related Glycine Depletion. Cell Rep 33, 108375. 10.1016/j.celrep.2020.108375. [PubMed: 33176135]
59. Yan-Do R, and MacDonald PE (2017). Impaired "Glycine"-mia in Type 2 Diabetes and Potential Mechanisms Contributing to Glucose Homeostasis. Endocrinology 158, 1064–1073. 10.1210/en.2017-00148. [PubMed: 28323968]
60. Dasarathy S, Kasumov T, Edmison JM, Gruca LL, Bennett C, Duenas C, Marczewski S, McCullough AJ, Hanson RW, and Kalhan SC (2009). Glycine and urea kinetics in nonalcoholic steatohepatitis in human: effect of intralipid infusion. Am J Physiol Gastrointest Liver Physiol 297, G567–575. 10.1152/ajpgi.00042.2009. [PubMed: 19571235]
61. Zeng X, Xing X, Gupta M, Keber FC, Lopez JG, Lee YJ, Roichman A, Wang L, Neinast MD, Donia MS, et al. (2022). Gut bacterial nutrient preferences quantified in vivo. Cell 185, 3441–3456.e3419. 10.1016/j.cell.2022.07.020. [PubMed: 36055202]
62. Giustarini D, Dalle-Donne I, Milzani A, Fanti P, and Rossi R (2013). Analysis of GSH and GSSG after derivatization with N-ethylmaleimide. Nat Protoc 8, 1660–1669. 10.1038/nprot.2013.095. [PubMed: 23928499]
63. Su X, Lu W, and Rabinowitz JD (2017). Metabolite Spectral Accuracy on Orbitraps. Anal Chem 89, 5940–5948. 10.1021/acs.analchem.7b00396. [PubMed: 28471646]

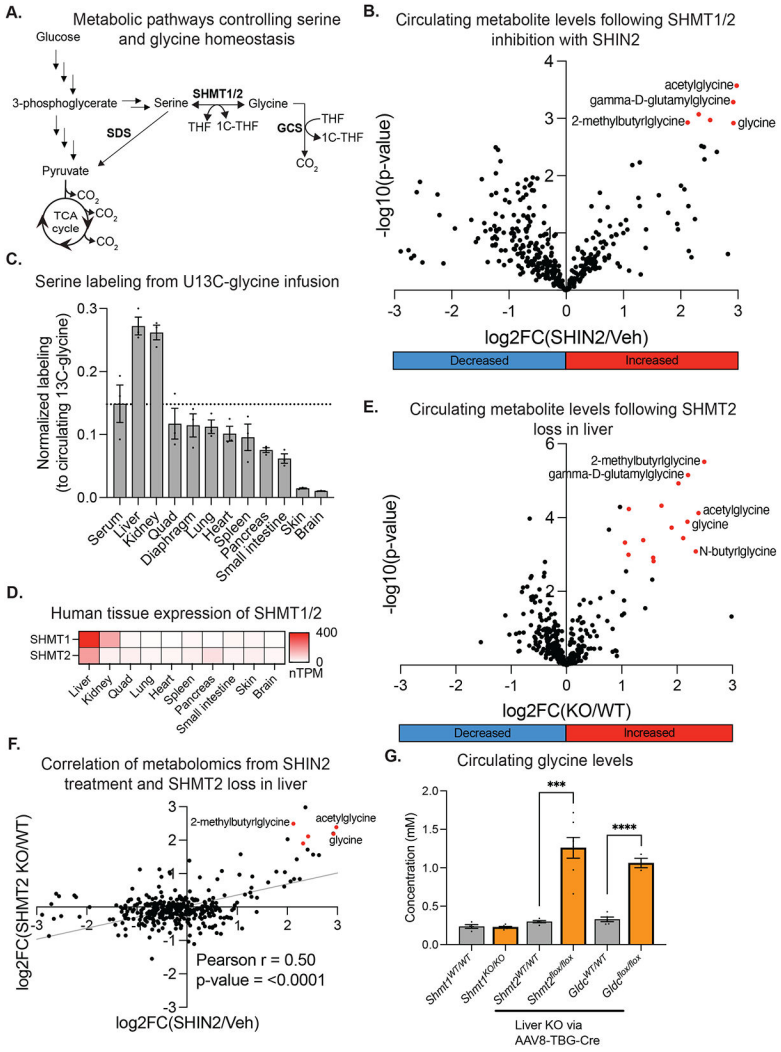

Figure 1: Hepatic SHMT2 is required for glycine clearance.

(A) Serine and glycine production and consumption pathways. (B) Serum metabolomics from C57BL/6 mice treated with vehicle or SHIN2 (n=3). (C) Normalized serine labeling from U13C-glycine infusion in circulation and tissues for fed mice (n=3). (D) Gene expression level of SHMT1 and SHMT2 across tissues in humans. (E) Serum metabolomics from C57BL/6-Shmt2$^{flox/flox}$ mice upon inducing SHMT2 liver knockout by AAV8-TBG-Cre viral infection (n=5-7). (F) Pearson correlation analysis of serum metabolomics from (B) and (E). (G) Serum glycine concentrations from C57BL/6 mice with whole-body SHMT1, liver-induced SHMT2 or liver-induced GLDC gene knockout (n=3-7). All data are reported as mean ± SEM, p value by unpaired T test (*<0.05, **<0.01, ***<0.001, <0.0001) and replicates (n) indicated. Metabolomics data underwent Benjamini-Hochberg correction for multiple comparison testing. See also Figure S1 and Table S1.

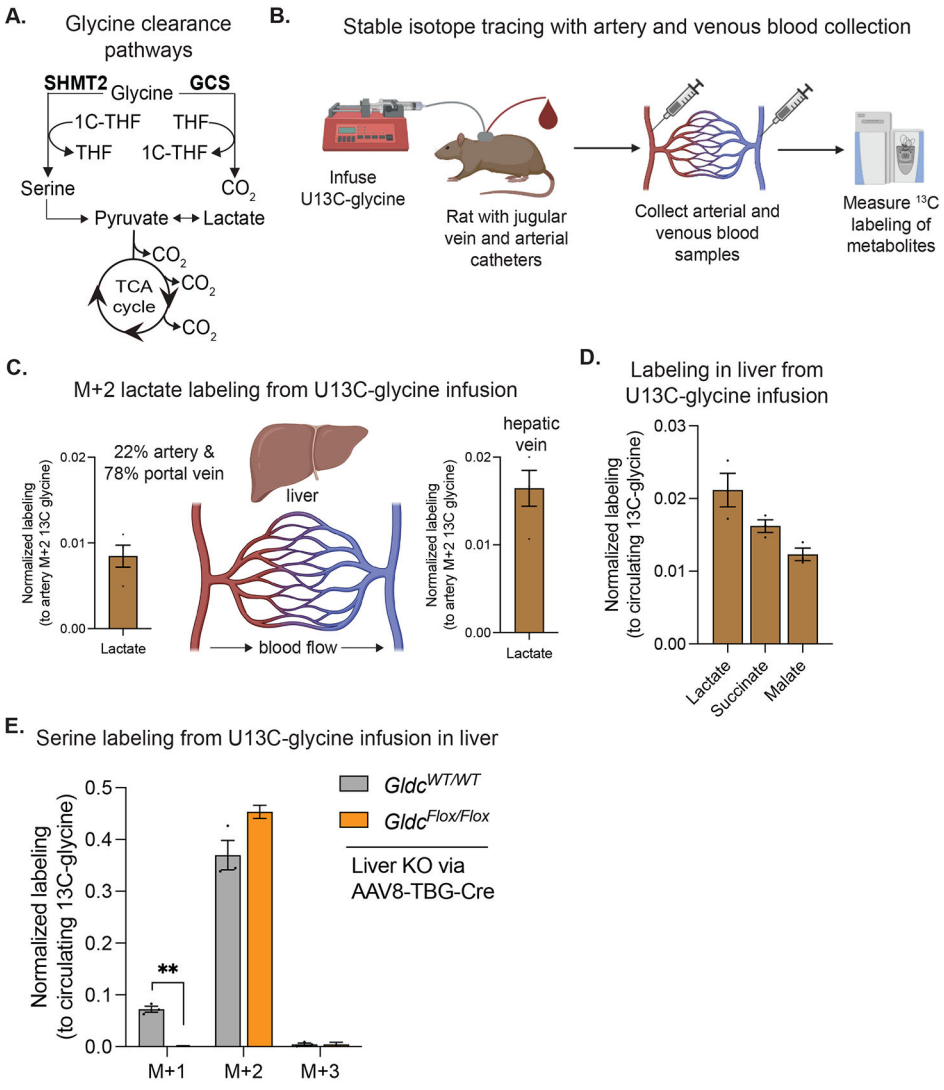

Figure 2: Reverse SHMT2 flux clears glycine by TCA oxidation in liver.

(A) Pathways of glycine consumption. (B) Experimental diagram for artery and venous sampling following stable-isotope tracing in rats. (C) Artery and venous lactate labeling from U13C-glycine infusion in Sprague Dawley rats (n=4). (D) Normalized labeling from U13C-glycine infusion of lactate, succinate and malate in liver for fed mice. (E) Normalized serine labeling from U13C-glycine infusion in liver of wild-type and liver GLDC knockout mice (n=3). All data are reported as mean ± SEM, p value by unpaired T test (*<0.05, **<0.01, ***<0.001, <0.0001) and replicates (n) indicated. See also Figure S2.

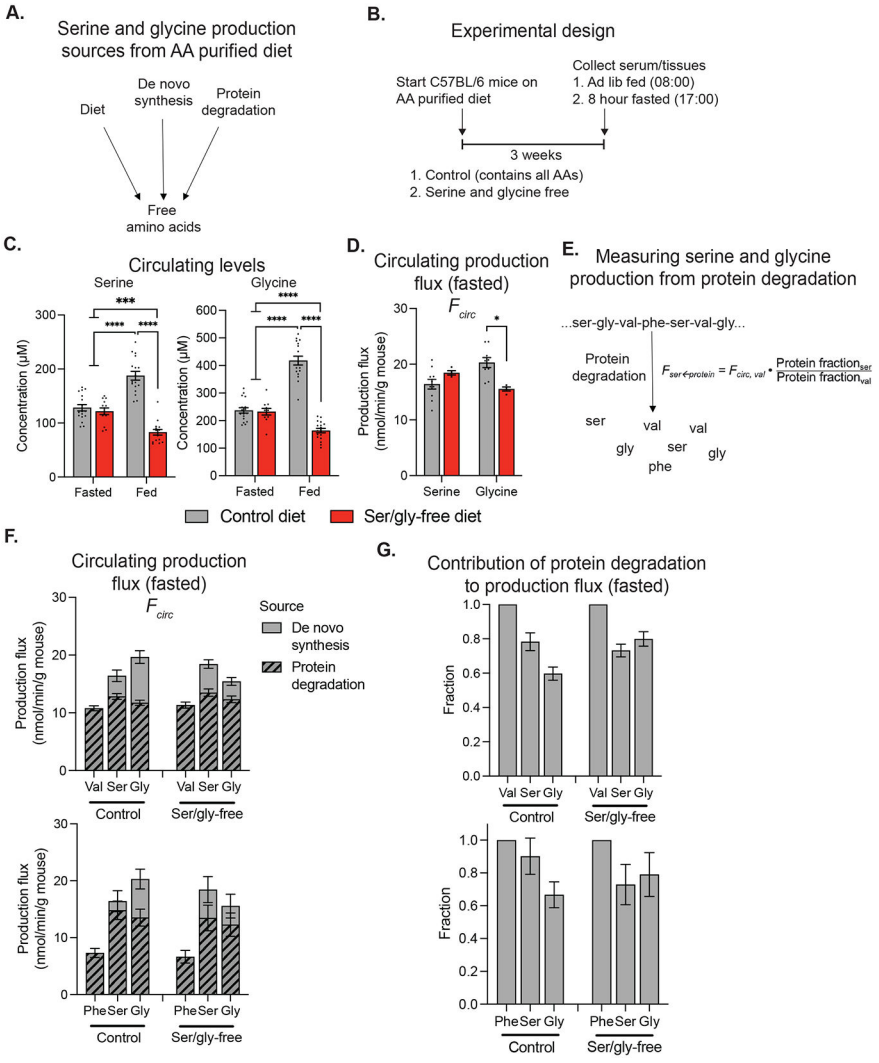

Figure 3: Diet-induced changes in circulating serine and glycine levels are lost in the fasted state when protein degradation is the major production source.

(A) Schematic of free amino acid sources when mice consume a purified diet. (B) Experimental design. (C) Serum serine and glycine concentrations (n=13-17). (D) Serine and glycine turnover fluxes for fasted mice on control or ser/gly-free diet (n=4-8). [U-^{13}C]serine tracer (30 mM) was infused at a rate of 0.1 μL/min/g mouse resulting in average circulating serine labeling fraction of 0.15 (control) and 0.14 (ser/gly-free). [U-^{13}C]glycine tracer (40 mM) was infused at a rate of 0.1 μL/min/g mouse resulting in average circulating glycine labeling fraction of 0.16 (control) and 0.20 (ser/gly-free). (E) Method for quantifying serine or glycine production from protein degradation based on production flux of an essential amino acid (valine or phenylalanine) and estimated amino acid abundance in protein based on codon frequency. (F) Valine, phenylalanine, serine, and glycine turnover fluxes for fasted mice on control or ser/gly-free diet (n=2-10). (G) Fraction of circulating valine, phenylalanine, serine and glycine production from protein degradation. All data are reported as mean ± SEM, p value by unpaired T test (*<0.05, **<0.01, ***<0.001, <0.0001) and replicates (n) indicated. See also Figure S3.

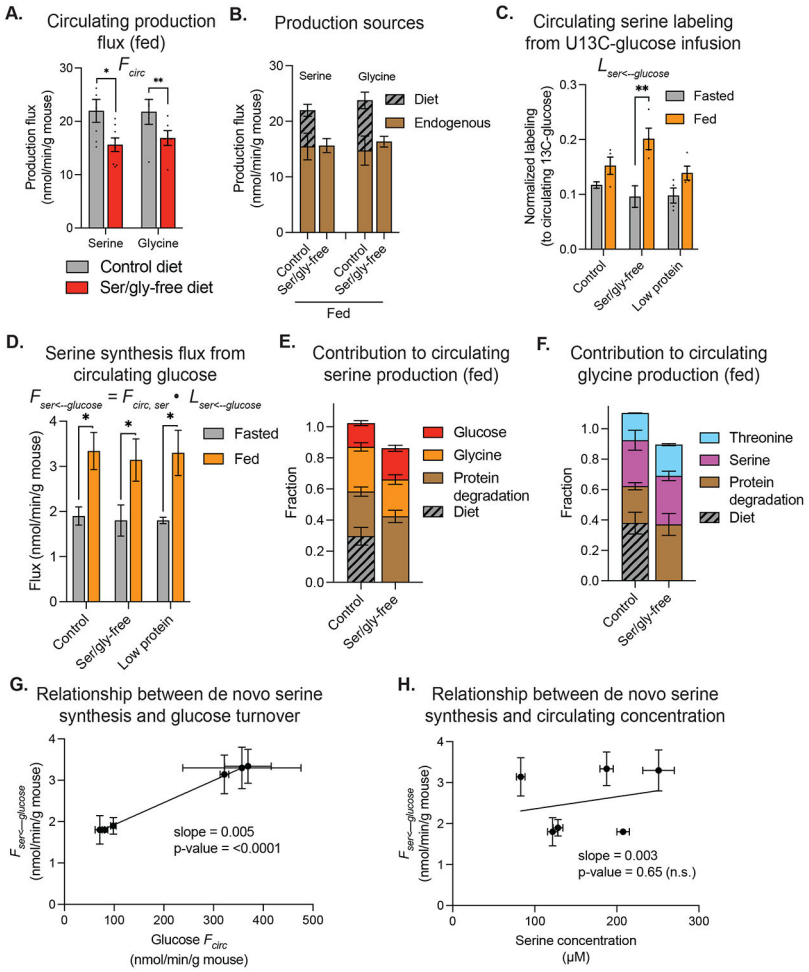

Figure 4: Feeding increases de novo serine synthesis from circulating glucose independent of serine levels.

(A) Serine and glycine turnover fluxes for fed mice on control or ser/gly-free diet (n=7-9). Serine tracer (30 mM) was infused at a rate of 0.1 μL/min/g mouse resulting in average circulating serine labeling of 0.12 (control) and 0.16 (ser/gly-free). Glycine tracer (40 mM) was infused at a rate of 0.1 μL/min/g mouse resulting in average circulating glycine labeling of 0.14 (control) and 0.20 (ser/gly-free). (B) Proportion of serine and glycine production fluxes from diet and endogenous sources for fed mice on control or ser/gly-free diet. Incoming flux from diet was subtracted from total turnover flux (F_{circ}) to determine endogenous fux. (C) Normalized serine labeling in circulation from U13C-glucose infusion. (D) De novo serine synthesis flux from circulating glucose. (E, F) Fraction of circulating (E) serine and (F) glycine production from each source for fed mice on control or ser/gly-free diet. (G) Relationship between de novo serine synthesis flux and glucose turnover flux. (H) Lack of relationship between de novo serine synthesis flux and circulating serine concentration. All data are reported as mean ± SEM, p value by unpaired T test (*<0.05, **<0.01, ***<0.001, <0.0001) and replicates (n) indicated. See also Figure S4.

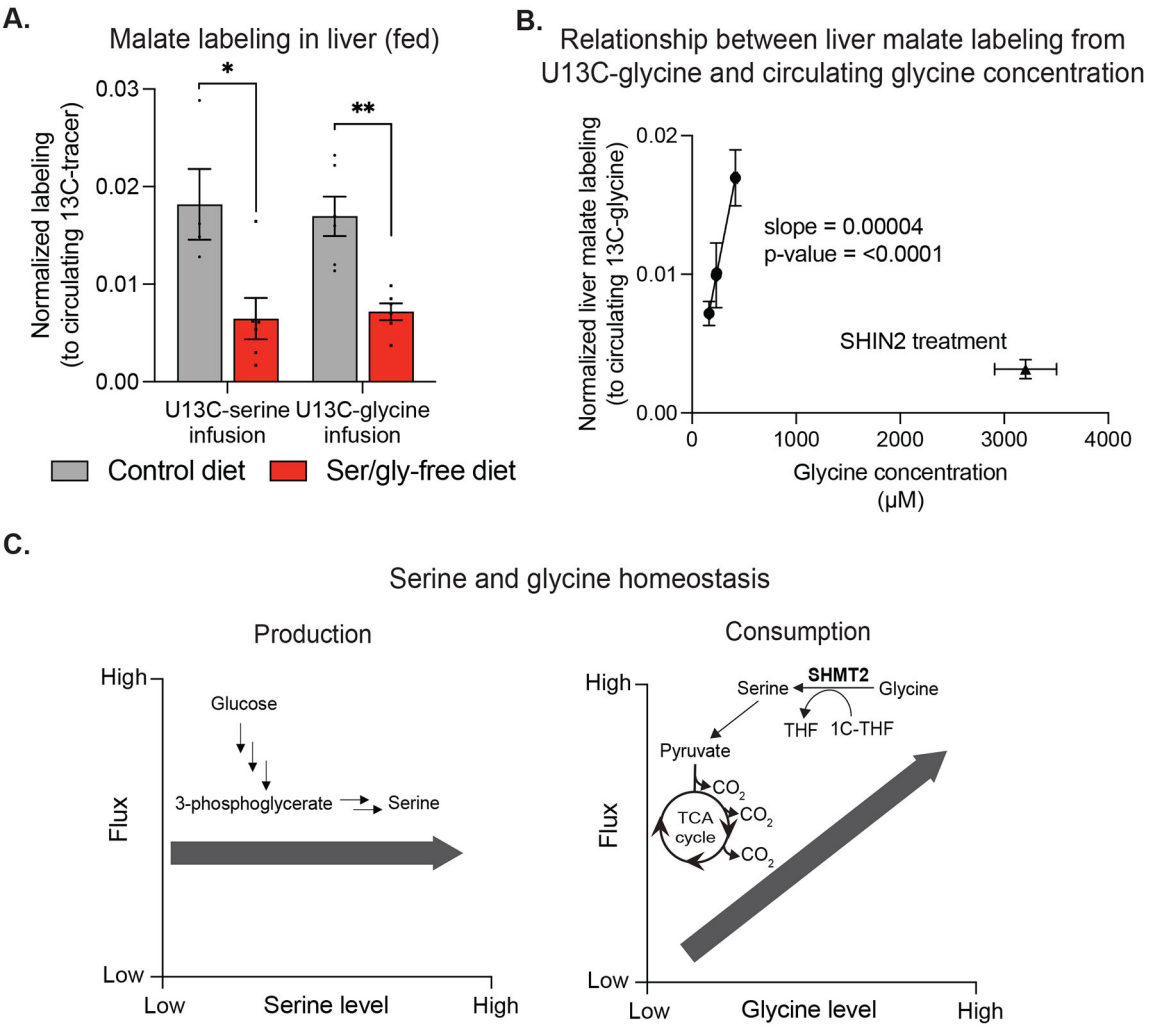

Figure 5: Serine and glycine homeostasis is achieved by mass-action driven TCA oxidation.

(A) Normalized labeling from U13C-serine and U13C-glycine infusions of malate in liver for fed mice on control or ser/gly-free diet (n=4-6). (B) Relationship between U13C-glycine labeling of liver malate and circulating glycine concentration in mice across dietary conditions compared to mice treated with SHIN2. (C) Schematic of production from de novo serine synthesis (left) and SHMT2-mediated glycine consumption (right) pathways and the relationship of these pathway fluxes with varying serine and glycine levels. Proportionality between consumption flux and concentration drives homeostasis. All data are reported as mean ± SEM, p value by unpaired T test (*<0.05, **<0.01, ***<0.001, <0.0001) and replicates (n) indicated. See also Figure S5.

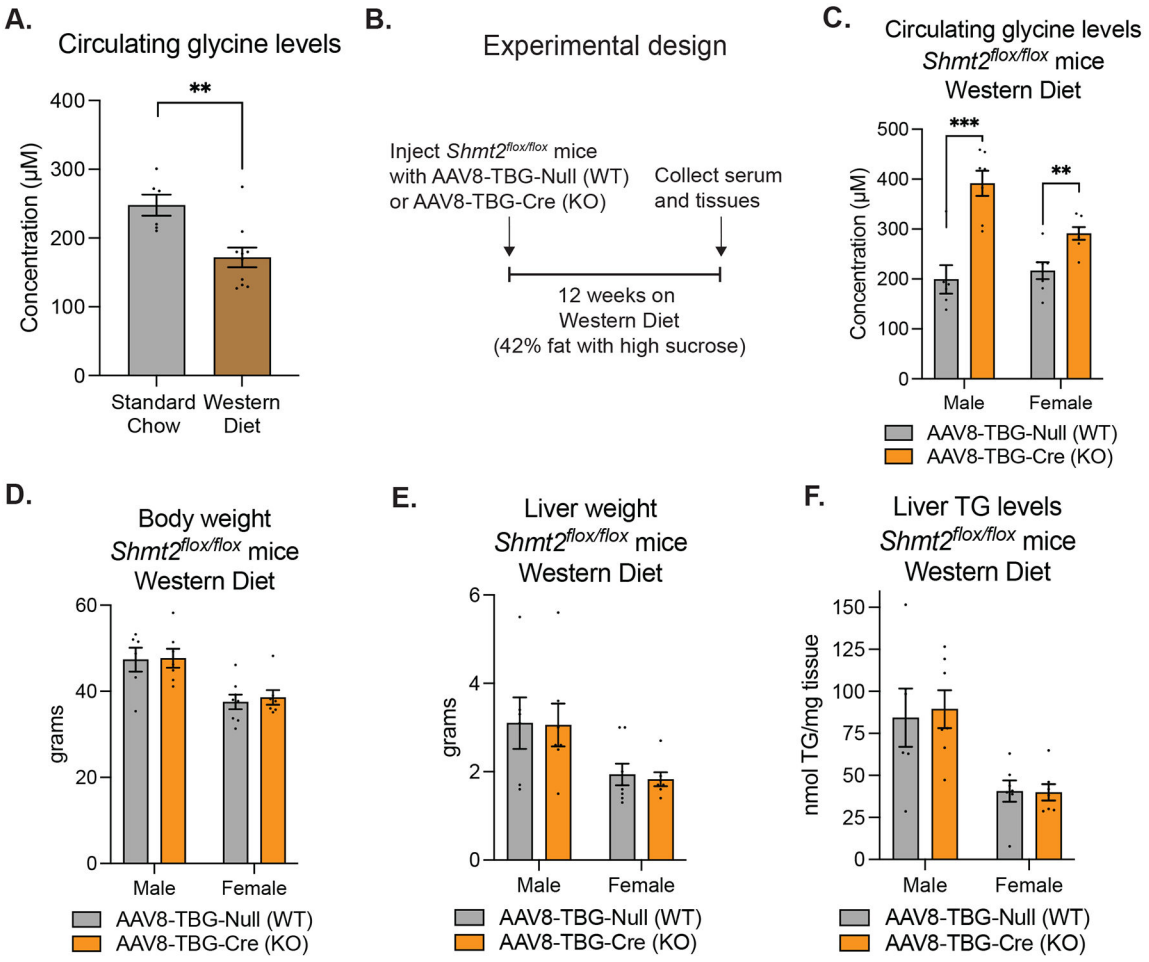

Figure 6: Elevating glycine levels by hepatic SHMT2 loss has no impact on diet-induced hepatic steatosis.

(A) Circulating glycine concentration of male C57BL/6 mice after 12 weeks on standard chow or western diet (42% fat with high sucrose) (n=6-10). (B) Experimental design for testing impact of hepatic Shmt2 on diet-induced liver steatosis. (C) Circulating glycine concentration, (D) Body weight, (E) Liver weight, and (F) Liver TG level of male and female mice after 12 weeks on western diet with or without hepatic Shmt2 liver knockout (n=6-8). All data are reported as mean ± SEM, p value by unpaired T test (*<0.05, **<0.01, ***<0.001, <0.0001) and replicates (n) indicated. See also Figure S6.